

QUANTIFYING DISPLACEMENT: A GENTRIFICATION'S CONSEQUENCE VIA PERSISTENT HOMOLOGY

RITA RODRÍGUEZ VÁZQUEZ¹ AND MANUEL CUERNO^{2, A}

ABSTRACT. Gentrification is the process by which wealthier individuals move into a previously lower-income neighbourhood. Among the effects of this multi-faceted phenomenon are rising living costs, cultural and social changes—where local traditions, businesses, and community networks are replaced or diluted by new, more affluent lifestyles—and population displacement, where long-term, lower-income residents are priced out by rising rents and property taxes. Despite its relevance, quantifying displacement presents difficulties stemming from lack of information on motives for relocation and from the fact that a long time-span must be analysed: displacement is a gradual process (leases end or conditions change at different times), impossible to capture in one data snapshot. We introduce a novel tool to overcome these difficulties. Using only publicly available address change data, we construct four cubical complexes which simultaneously incorporate geographical and temporal information of people moving, and then analyse them building on Topological Data Analysis tools. Finally, we demonstrate the potential of this method through a 20-year case study of Madrid, Spain. The results reveal its ability to capture population displacement and to identify the specific neighbourhoods and years affected—patterns that cannot be inferred from raw address change data.

1. INTRODUCTION

Population displacement, a housing-related involuntary residential dislocation [34] is one of the main symptoms of gentrification. Ruth Glass, who coined the term gentrification in her 1964 book “London: Aspects of Change” [28], already observed that gentrification was pushing lower income people and small businesses away from their original locations. The widespread and uneven effect of displacement across social groups has motivated a broad range of studies, focussing on everything from characterising displaced individuals to identifying the potential causes and consequences of the phenomenon.

A wide range of approaches has been employed to assess the extent of displacement in gentrifying areas. Survey-supported research detects displacement by explicitly inquiring about individuals’ motivations for relocation. The seminal 1981 study conducted by the National Institute of Advanced Studies [21] examined who and why was moving out of the rapidly uplifting neighbourhood of Hayes Valley in San Francisco. Researchers found that about one fourth of the movers between 1975–1979 left involuntarily, and were mainly black, elder or poor. More recent studies [19, 18] analyse the prevalence and characteristics of displacement using Milwaukee Area Renters Study survey data. The elevated costs and limited availability of survey data have encouraged alternative methods

Date: December 12, 2025.

2020 Mathematics Subject Classification. 30L15, 53C23, 53C20, 55N31.

Key words and phrases. Gentrification, Persistent homology, Displacement, Topological Data Analysis, Cubical complex.

¹ Department of Quantitative Methods, CUNEF Universidad, Madrid, Spain. rita.rodriguez@cunef.edu.

² Department of Mathematics, CUNEF Universidad, Madrid, Spain. manuel.mellado@cunef.edu.

^A M. Cuerno has been financially supported by the project “Charting political ideological landscapes in Europe: Fault lines and opportunities (POL-AXES)” - Programa Primas y Problemas 2023 from Fundación BBVA, and PID2021-124195NB-C32 and PID2024-158664NB-C22 from the Ministerio de Economía y Competitividad de España (MINECO).

that infer displacement indirectly through socio-economic indicators, either by contrasting these measures between in-movers and out-movers or interpreting spikes as evidence of displacement. For instance, [24] investigates exit rates of low-income residents in neighbourhoods with increasing income, while McKinnish et al. [35] focus on exit rates among vulnerable groups. Other studies compare a metrics’s value in a neighbourhood with that in a control group: Ding et al. [20] contrast mobility rates and destination outcomes between gentrifying and non-gentrifying tracts in Philadelphia, and Ellen et al. [23] compare demographic changes in gentrifying tracts with those in the metropolitan area to assess whether observed shifts indicate displacement or citywide dynamics. Finally, composite indices such as the Los Angeles Index of Displacement Pressure [38] weigh individual, household, and neighbourhood indicators to assess relative risk.

These approaches present a series of shortcomings, which fall into two categories. The first and perhaps the most important one is the lack of replicability to other cities and time periods, which is due to ad-hoc methodologies and data. Specifically, the choice of a metric and a control group lead to different definitions thereof, hindering the comparison of displacement rates, and surveys and specific indicators are tailored to the specific cities they are designed for, such as the Los Angeles Index of Displacement Pressure. Second, the time-scale of some analysis is too short to capture the full displacement processes, as not all leases expire at the same time, and to allow to establish the relationship between gentrification and displacement, as one ought to determine whether the displacement was already taking place prior to the gentrification process.

We propose a novel methodology to overcome these challenges and validate it in a case study for the city of Madrid, Spain. Using solely address change data—which is not tied to any city-specific features and is publicly available—we build a suitable topological space and apply persistent homology, a key tool in Topological Data Analysis (TDA), to quantify displacement.

To the best of our knowledge, this is the first application of TDA techniques to gentrification and its consequences. Nevertheless, related literature employs persistent homology to study urban factors potentially reinforcing gentrification processes. From the standpoint of resource access, Hickok et al. [30] developed a methodology to analyse access to polling sites in several major U.S. cities, while O’Neil and Tymochko [36] conducted a similar study focused on access to cooling centres; Tymochko is also currently extending the methodology of [30] to the case of urban parks. More politically oriented applications include the work of Friesen and Ziegelmeier [26] on racial segregation in the U.S., and Duchin et al. and Shah [22, 39] on gerrymandering. From a methodological perspective, other works—such as [1]—have used 3D solid bodies constructed from cubical complexes for TDA purposes, but without incorporating time as one of the axes. Therefore, the present work is novel both in its content and in its methodological approach.

This work opens the door to applying the same methodology to measure displacement in cities around the world. The data we use is collected in most countries, making our approach highly replicable. Taken together, these features address the two main critiques identified in the existing literature: the reliance on ad-hoc techniques and data and inadequate time-scale. In addition, the use of persistent homology makes our contribution both novel within the TDA framework and well grounded, as it relies on a construction tailored to this problem that fully exploits the strengths of persistent homology.

2. MATERIALS AND METHODS

2.1. Data. The city of Madrid organised into multiple administrative levels. It comprises 21 districts numbered 1 to 21 (see Figure 1), each subdivided into several neighbourhoods. Each one is uniquely identified by a numerical code in which the final digit denotes the neighbourhood and the preceding digits indicate the district. For example, 26 designates the 6th neighbourhood in district 2, and 141 denotes the 1st neighbourhood in district 14. In order to incorporate the spatial

structure of these neighbourhoods into our study, we use a shapefile of the city neighbourhoods, available at [5].

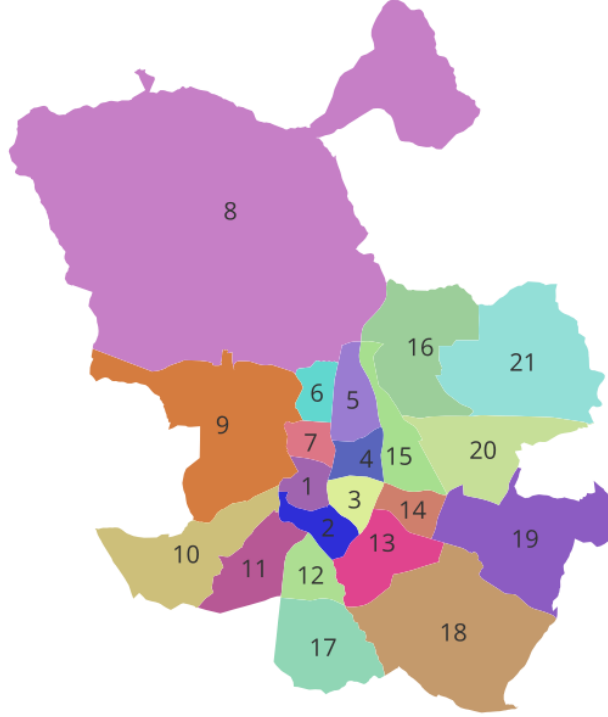


FIGURE 1. Madrid map and their 21 districts as of April 2025.

All the data used in this study is publicly available on the official website of the city council [4]. The main data sources are the tables in the ‘C. Demografía y Población’ section, specifically those containing information about address changes with origin inside the city. This includes information on the number of residents who moved, their destination and the number of people who left the city. We use the finest spatial and temporal granularity available, which is yearly data at neighbourhood level. Each year’s data may be represented as an origin-destination matrix, whose rows and columns represent the possible origins and destinations, respectively, for residents who moved that year. Thus, rows correspond exactly to the city neighbourhoods, whereas the columns include all the neighbourhoods together with other possible destinations for people moving outside the city. We consider the full time series available as of April 2025, i.e. data from 2004 until 2023.

2.2. Persistent homology. Homology is a central tool in Algebraic Topology: given a topological space X , its homology groups $H_n(X)$ encode n -dimensional holes, such as connected components ($n = 0$), loops ($n = 1$), and voids ($n = 2$). At the beginning of this century, topology began to play a key role in data analysis [43, 14, 44], giving rise to Topological Data Analysis (TDA). The central idea is to study the shape of data by analysing how topological features evolve as the scale changes; *persistent homology* is the primary tool for doing this. The birth and death of n -dimensional holes is tracked through a filtration: a nested family of simplicial complexes—combinatorial structures made of vertices, edges, triangles, and their higher-dimensional counterparts—built from point-cloud data by adding k -simplices as a scale parameter increases. The resulting features are summarised in barcodes or persistence diagrams, where each interval $[b, d]$ (or point (b, d)) indicates that the

feature appears at scale b and vanishes at d , where $b \leq d$ as they indicate ordered times. Points near the diagonal—when b is close to d —correspond thus to short-lived structures; see Figures 4 and 5, or the illustrative examples in [27]. For readers interested in formal definitions of homology, simplicial complexes, and related notions, we refer to [29].

2.3. Cubical complexes for grayscale images. The theory outlined in the previous section for simplices can be mimicked for n -dimensional cubes. This alternative approach, known as the *cubical complex* setting [43, 31, 41], is particularly well suited for the study and analysis of grayscale images [13, 16]. Figure 2 illustrates how a cubical complex can be obtained from a grayscale image by means of a 2-dimensional grid. The resulting 2-dimensional cubes are known as pixels in analogy to digital photography. These inherit the intensity values from the original image, yielding a natural filtration parameter. Pixels are introduced into the filtration process in order of decreasing intensity: darker regions appear first, followed progressively by lighter ones; see Figure 2. There are two main approaches to the construction of cubical complex filtrations, linked by a duality result [13] ensuring that both yield equivalent conclusions. In this paper, we adopt the one known as *T-construction*. We refer to the Supplementary Information (SI), Appendix B for a more detailed discussion.

2.4. Volume-type complexes for time-series data. To quantify population displacement in a manner that can be generalised to other cities, our approach relies solely on address change data and the city’s administrative division into neighbourhoods. This data undergoes the following preprocessing. We begin by dividing all individuals who moved in a given year into four groups according to their origin and destination. For each group, we then construct a three-dimensional cubical complex and compute its persistence. These cubical complexes encapsulate both the city geography and the temporal evolution of each population group.

Recall that our dataset spans 20 consecutive years, where each year’s data may be thought of as an origin-destination matrix whose entries are the number of people moving from a given neighbourhood to another area. We simplify these matrices by replacing all the possible destinations by the following summarised four ones: the same as the origin neighbourhood (from now on referred to as ‘stay’); a different neighbourhood within Madrid (‘city’); a different town or city in the Comunidad de Madrid, the region Madrid belongs to (‘C. Madrid’); and another region or country (‘outside’). Although each of these groups may be further divided, we opt for a consolidated approach to maintain simplicity and analytical efficiency. Finally, we normalise the resulting matrix so that each row sums to 1.

We construct a volume-cell complex for each of the groups described above so as they reflect the geography of the city neighbourhoods while simultaneously incorporating a temporal component. To do so, we leverage the fact that data in every year references the same geography up to minor changes; see §2.1 and SI. We start by building a 100×100 grid covering the city map, dividing the city into squares of the form $[x, x + 1] \times [y, y + 1]$, and then add a third dimension corresponding to the time. Since we have data for 20 consecutive years, this yields a $100 \times 100 \times 20$ grid. Notice that this grid is independent of the group. Fix now one of the four groups. We now define a 3-dimensional grayscale digital image \mathcal{I} of size $(100, 100, 20)$, associating to each tuple (x, y, z) the share of people moving from the region $[x, x + 1] \times [y, y + 1]$ in year z that fall into the given group. This yields four 3-dimensional images of the same size and sharing the same grid.

We now construct four filtered cell complexes following the T-construction. Fix one of the grayscale digital images. Its top-dimensional cells or *voxels* are the cubes constructed above, which correspond precisely to the elements in the 3-dimensional grid, and their lower-dimensional counterparts are all their faces, edges and vertices. We then construct a filtration V assigning to voxels the value from the grayscale image, and then extend it top-down to their faces, edges and vertices by assigning to them the smallest value of all the adjacent voxels. This yields four nested

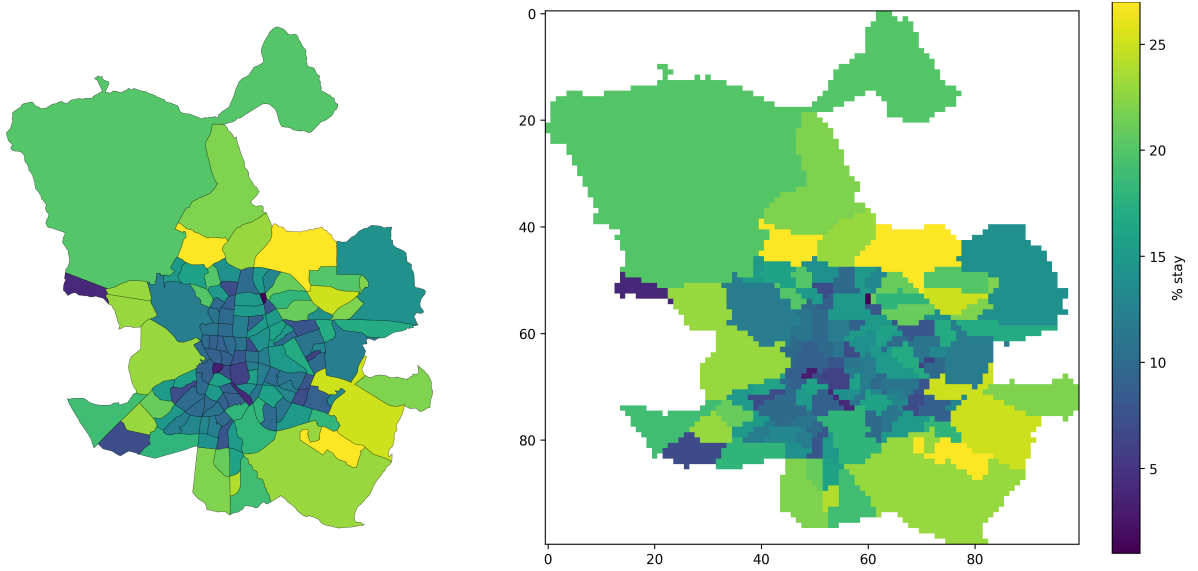


FIGURE 2. Grayscale image depicting the percentage of people moving in 2023 that stayed in the same neighbourhood (left) and resulting 100×100 covering the city map (right).

sequences of cubical complexes indexed by a parameter r ranging from 100 to 0: recall that for a fixed value r , a voxel c is selected if $V(c) \geq r$. The resulting filtered complexes preserve the neighbourhoods geography. For a more technical exposition of the T-construction, we refer the reader to the Appendix B.

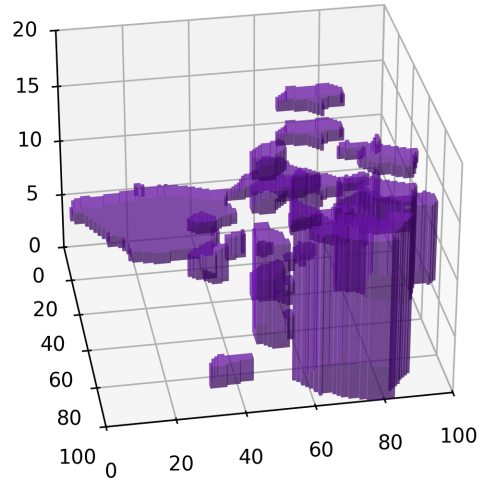


FIGURE 3. Example of the cubical complex for people moving that stayed in the same neighbourhood obtained by selecting the parameter value $r = 30$.

We then compute persistent homology for each of the four resulting filtered cell complexes using CubicalRipser, an extension of the Ripser Python library designed for cubical complexes [32]. The reason for this choice is three-fold: It supports the T-construction for cubical complexes, it is robust, and the output format provides not only the birth and death times of the topological features, but

also the coordinates (x, y, z) where they initiate and die. Notice that since we are working on a 3-dimensional grayscale image, we only consider the zeroth, first and second homology groups.

We can now represent the obtained persistent homology through its barcode, where the length of each bar depicts the lifespan of the corresponding feature; see Figure 4; or its persistence diagram; see Figure 5.

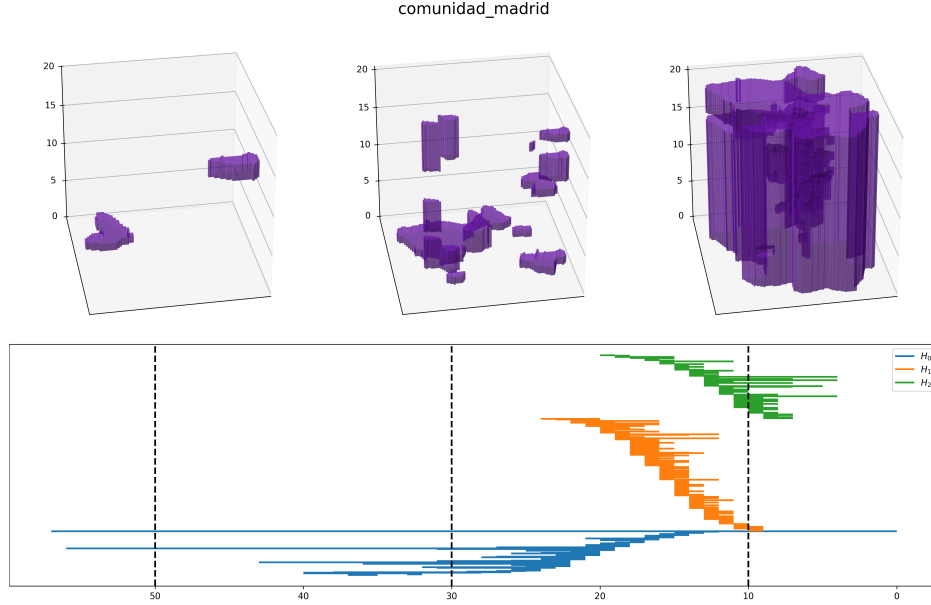


FIGURE 4. Example of developing persistence for the group of people that moved from Madrid to another city within the same region. The three images at the top row show the cubical complexes for people who moved from Madrid to another city within the same region obtained by selecting the parameter values $r = 10, 30$ and 50 . The bottom row shows the barcode obtained for this filtered complex, displaying the persistence of the connected components (H_0 features), topological loops (H_1 features) and of the cavities (H_2 features).

RESULTS

Identifying potentially displaced individuals. Displacement is typically defined in terms of residents’ reasons for moving—information that is difficult to obtain directly and is therefore often inferred from aggregated socio-economic indicators. In the following, we explain how the four groups we classified movers into allow us to infer population displacement.

Groups are determined by the origin and destination of each move. The underlying assumption is that people develop social and practical ties where they live, such as places of study, family and friends, and distance might weaken that social network [10, 33]. Hence, individuals who relocate often prefer to remain near their previous area of residence. We encoded this preference as follows. The go-to option would be to move within the same neighbourhood, followed by moving to another one within the city.

The housing market in Madrid is highly tensioned. According to official statistics, between December 2019 and December 2024 the average rent price per square metre in Madrid has increased 24,64%, see [4] section ‘E. Edificación y Vivienda’. It is a well-established fact that housing prices impact migration flows. A study on migration and housing markets conducted by the OECD concluded that high housing costs discourage staying or moving into a region [15]. This pattern

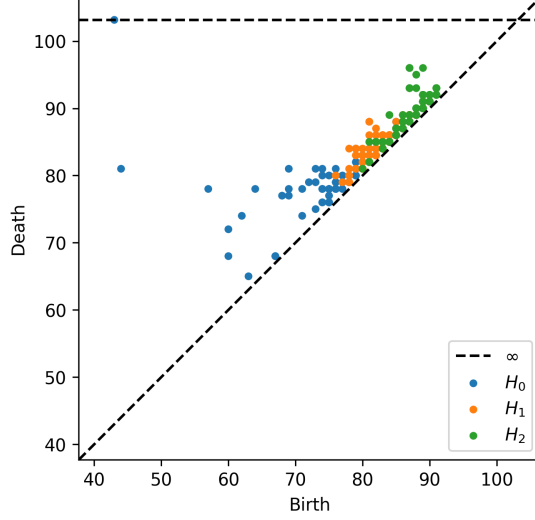


FIGURE 5. Persistence diagram of the filtered complex for the group of people who moved from Madrid to another city within the same region, displaying the H_0 , H_1 and H_2 features. Points close to the diagonal present low persistence.

supports the idea that the search for more affordable housing is the most likely driver of moves out of the city, allowing us to infer population displacement. We consider two destinations for people who move out of the city: another town within the same region and outside the region, staying in the same region being the preferred option among them, as it will likely allow them to maintain some of their social and economic ties, such as their jobs.

Meaning of topological features. Let us now illustrate how TDA can help us extract such patterns. Our approach examines the “shape” of the data for each group—in particular, how the residents of Madrid’s neighbourhoods moved over a 20-year period, by means of the persistent homology of the four cubical complexes described above. We therefore explain how the resulting topological features may be interpreted.

Recall that our data is 3-dimensional, so we need to consider all homology groups up to the second. This is a direct consequence of simultaneously considering the geography of the city and the temporal component. Analysing, for example, one year at a time would yield a lower-dimensional complex and thus a trivial H_2 . We shall exploit this richness.

Consider one of the four groups. Features in H_0 correspond to enclaves of people moving to that particular destination. Specifically, if such an enclave is born at filtration-value r , it means that the prevalence of that group is r . Such enclaves may span several consecutive years, possibly comprising different neighbourhoods across that time period. Consider, for instance, two adjacent neighbourhoods, A and B. A feature in H_0 could consist of neighbourhood A in year 1, A and B in year 2 and B in year 3. Thus, in years 1 and 3 the enclave consists of mutually exclusive sets of neighbourhoods.

Highly persistent H_0 features are relevant enclaves for that group. Specifically, a connected component born at filtration-parameter value r presents a prevalence of $r\%$ of the group, and its death time indicates at which point it is fused with another (older) enclave. Thus, its persistence indicates how relevant that enclave is compared to close ones. In particular, the most prominent H_0 feature corresponds to the neighbourhood and year with the highest concentration of that group, which corresponds to its birth time. As it never fuses to another enclave, its death time is 0, the lowest possible value for r . Recall that in our setting, the filtration parameter goes from 100 to 0.

		stay	city	C. Madrid	outside
# features	H0	73	98	80	75
	H1	209	211	197	201
	H2	66	40	41	55
# important features	H0	35	54	34	39
	H1	66	84	23	44
	H2	23	19	10	19

TABLE 1. Number of topological features in each group. Important features are those with persistence > 2 .

While homology classes in H_0 correspond to connected components, H_1 ones represent crossing-through holes within those enclaves, and H_2 ones cavities inside those enclaves, or non-crossing-through holes. Both indicate that the given group is not prominent there and that instead the rest of the groups are concentrated there. To illustrate the difference between the two, consider a neighbourhood A that is fully surrounded by other city neighbourhoods—not located at the border of the city—together with all its adjacent neighbourhoods, over a period of three consecutive years. On the one hand, if an enclave consists of only all those neighbourhoods except A over all three years, then we have an H_1 feature. On the other hand, if neighbourhood A is only missing in the middle year, then we have an H_2 feature. The former situation suggests that something in A is different from its adjacent neighbourhoods, as the hole is maintained over time, and the latter that this phenomenon is restricted to a specific period of time. Analogous examples may be built exchanging the time and space variables. In general, 1-dimensional holes point at phenomena that are not bounded to part of the space or to time periods present in the enclave, whereas 2-dimensional ones indicate that the phenomenon is bounded to a specific area and period.

Persistence of H_1 and H_2 features indicates how long it takes for that hole to be closed. Hence, persistent H_1 and H_2 features suggest that the neighbourhoods and years belonging to that hole present different characteristics from close-by neighbourhoods and years, which drive individuals to behave differently. Remark that persistence of topological features cannot be observed by means of statistical methods.

Findings. We examine the topological features obtained for each of the four groups. Tcrisper provides the xyz coordinates of birth and death of each feature, so we can trace them back to specific neighbourhoods and years. However, while birth places are relevant for H_0 features, further developments are needed to fully exploit the topology of 3-dimensional grayscale images. Specifically, we extract which neighbourhoods and years make up a connected component at a given filtration-parameter value; and to gain insight into displacement from 2-dimensional features, we compute which neighbourhoods and years are contained in each cavity at birth time. TCripper outputs require a cleaning process prior to analysis, as they often contain duplicate rows in H_1 and H_2 . Additionally, our development described above revealed that some reported “distinct” cavities—despite being associated with different birth or death voxels—were composed of exactly the same underlying set of voxels. All of these have been removed from our analysis.

Let us first analyse the H_0 features. In the group ‘stay’, the most persistent one originates in 2009 in neighbourhood ‘27 Atocha’, which spans the area between the main train station Atocha and Méndez Álvaro, an important transportation hub. This highlights a difference in the population dynamics compared to the surrounding areas and years. While this feature requires a while to expand, others born around the same time quickly span several years and neighbourhoods. Nevertheless, we observe that it is only at high values of the filtration-parameter that the connected

components in this group expand vertically beyond the 2020 threshold or include neighbourhoods in the ‘01 Centro district’, the historic centre. These facts denote population displacement subject to temporal and spatial constraints.

The city group exhibits more connected components than the others (see Table 1), indicating limited spatial and temporal concentration. Its two most persistent H_0 features both arise in neighbourhood ‘27 Atocha’ and expand later, forming stacked components interrupted in 2009–2010—when the stay H_0 feature emerges; see Figure 6. This pattern reflects a preference for intra-neighbourhood moves when market conditions permit, as after the 2008 financial crisis.

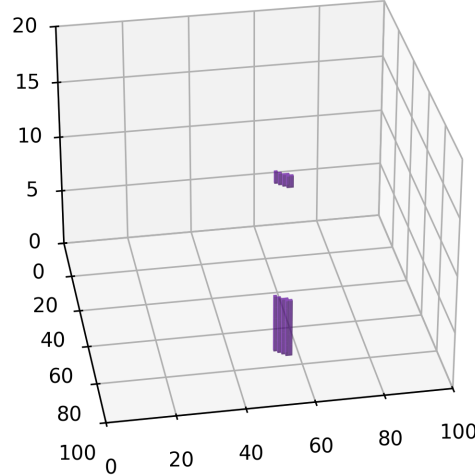


FIGURE 6. First two connected components born in the group ‘city’. Both cover only the neighbourhood 27 Atocha.

In the ‘Comunidad de Madrid’ group, the first connected components are born at the city border in distant neighbourhoods and first expand to further years, i.e., along the vertical axis, resulting in high persistence. They do not necessarily imply substantial displacement, as residents may simply relocate within the immediate vicinity. In contrast, H_0 features in the ‘outside’ group mark displacement. We identify that neighbourhood ‘141 Pavones (East)’ has undergone high pressure, as several of the most persistent features are born there. The rapid, citywide expansion of highly persistent features after 2016 likewise suggests that displacement has become more intense and widespread in recent years.

Higher dimensional topological features contribute to identifying displacement as follows: 1– and 2–holes in the groups ‘stay’ and ‘city’ suggest displacement, whereas those in ‘Comunidad de Madrid’ and ‘outside’ a stable market, especially if accompanied by a ‘stay’ or ‘city’ 0–feature contained or largely overlapping the cavity. It should be noted that H_2 features hold greater importance and convey more comprehensive information on displacement than H_1 ones.

All four groups have a high number of low persistent H_1 features. The group ‘stay’ presents the most persistent 1–hole, whose birth and death hint at population displacement in the north-eastern part of the city (districts ‘20 San Blas-Canillejas’ and ‘15 Ciudad Lineal’) in 2016–2019. The ‘city’ group’s two most persistent H_1 features both emerge and dissolve near the airport (district ‘21 Barajas’), revealing displacement in overlooked peripheral areas. The two remaining groups show little H_1 persistence, providing less insight into population displacement. The features in the ‘Comunidad de Madrid’ group are spatially and temporally spread-out, unlike the localised ‘outside’ group ones. The latter, specifically the feature located in the highly touristified ‘01 Centro’ district

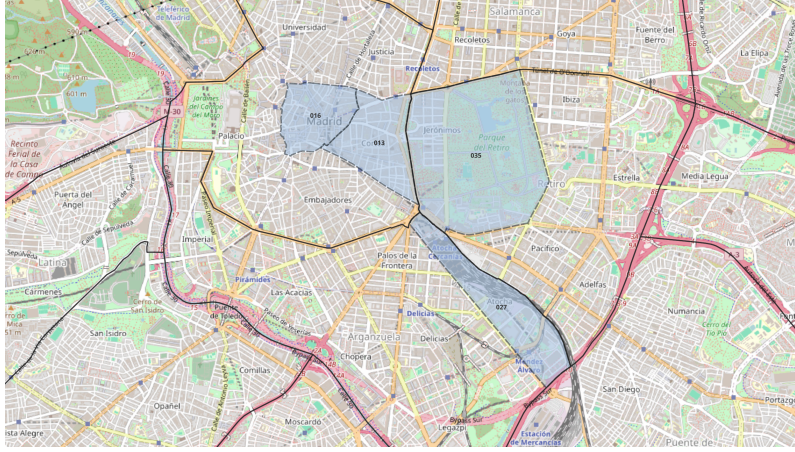


FIGURE 7. Map of central-south Madrid with neighbourhoods 13, 16, 27 and 35 highlighted. District boundaries are outlined in solid lines and neighbourhood limits by dashed lines.

during the 2020-2021 COVID pandemic, exemplifies a housing market relaxation and demonstrates our approach’s ability to capture subtle population displacement patterns.

We now examine H_2 features, which may exhibit complex dynamics. Note that cavities often emerge as “nested bubbles” within or around existing ones, dying at varying filtration values. For instance, a feature born from another’s split will have different birth and death times.

The three most persistent H_2 features in the group ‘stay’ are nested, with the middle one being most persistent. At birth, the central cavity covers central districts (1-11) from 2013 onwards, intensely affecting neighbourhoods 13, 16, 27 and 35; see Figure 7. We conclude that significant population displacement occurred in the central city area since 2013, coinciding with the post-2008 crisis recovery, and hit the areas between Sol and the Atocha train station the hardest.

The group ‘city’ presents the most persistent 2–hole of all groups, which spans a substantial area of the city. This large-scale cavity, with 110 out of 131 neighbourhoods present at birth, results from the merging of simultaneously formed connected components. The third most persistent feature, nested within this first one, is particularly notable as it is confined to neighbourhood 27 during 2020-2021, signaling a bounded decrease in housing market tension in a highly affected area, likely triggered by the pandemic. This illustrates the method’s ability to identify both large-scale and localised, temporary population dynamics.

The H_2 features in the group ‘Comunidad de Madrid’ and especially in ‘outside’ identify areas of reduced displacement. The top three features in both groups are nested and shrink quickly, making specific long-appearing neighbourhoods our primary interest. In the ‘outside’ group, these encompass districts in the south-east of the city: ‘13 Puente de Vallecas’, ‘15 Ciudad Lineal’ and ‘18 Casco Histórico de Vallecas’; see Figure 8. No neighbourhood appears after year 2019, signaling a generalized city-wide pressure thereafter. In ‘Comunidad de Madrid’, the most interesting cavity is the third most persistent one, comprising only neighbourhood ‘27 Atocha’ during 2006-2009. This offers additional evidence of the unique dynamics characterising this area.

The analysis of the topological features of the four groups revealed particularities of displacement that cannot be seen from the raw data. We found that neighbourhood ‘27 Atocha’ is a key case study, and presents a different behaviour from its surroundings, demonstrated by persistent H_0 and H_2 features and cavities consisting only of this neighbourhood. Initially part of a stable market, marked by an H_2 feature in ‘Comunidad de Madrid’ and a following connected component in ‘stay’ arising after the financial crisis, its population dynamics shifted dramatically afterwards. Strong

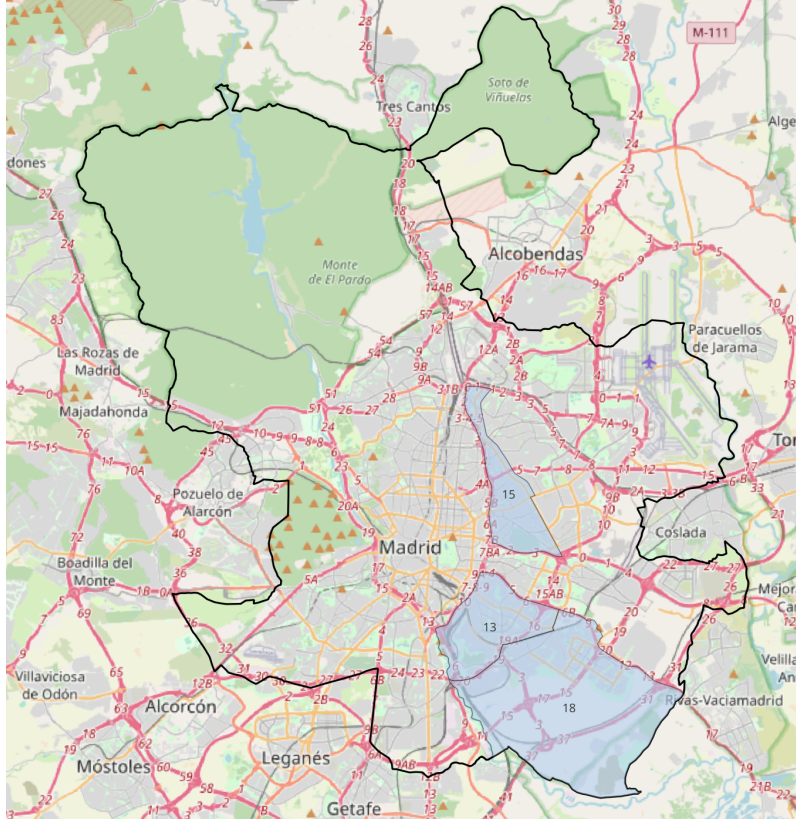


FIGURE 8. Map of Madrid with districts 13, 15 and 18 highlighted. City boundary is outlined in black.

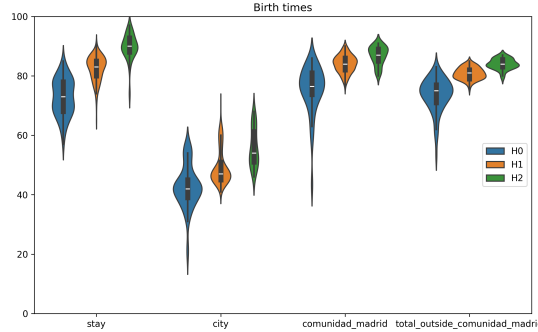


FIGURE 9. Distribution of the birth times of the topological features of each group, split by dimension.

displacement, marked by a persistent cavity in ‘stay’ from 2013-2023 containing it, was briefly interrupted during the COVID-19 pandemic, as shown by a ‘city’ cavity. This highlights the neighbourhood’s distinct responsiveness to market forces, which distinguishes it from its surroundings and acts as a focal point for broader area dynamics.

DISCUSSION

This study presents a novel method to quantify population displacement, a major toll of gentrification, and demonstrates that it reliably identifies displacement in a case study of the city of

Madrid, Spain. It effectively detects areas and times where people moved due to displacement. The split of the movers into four groups contributes particularly to this, as each group exhibits different motivations for moving. This method involves two main phases: the construction of suitable cubical complexes and the subsequent analysis of that complex through persistent homology. We leverage publicly available data to build the grayscale images underlying our cubical complexes: the geography of the administrative division of the city into neighbourhoods and address change data (yearly origin and destination of the city inhabitants moving). Persistent homology is a widely-used tool from Topological Data Analysis to synthesise the shape of data that is particularly robust to noise.

Prior attempts to quantify population displacement present both data and methodological limitations. Studies relying on ad-hoc metrics, surveys, or tailored to the city specifics hinder comparability, and oftentimes data availability restricts the analysis to short time spans. In contrast, our study only uses publicly available, periodically collected data, enabling replicability across cities, which, combined with persistent homology of the four cubical complexes, allows us to work on an adequate time scale. Methodologically, displacement studies often depend on a subjectively chosen control group, which strongly impacts their conclusions. Our approach overcomes this shortcoming by incorporating all neighbourhoods and all years into a single cubical complex, allowing persistent homology to extract topological patterns based on spatio-temporal proximity without requiring a control group.

Although our approach offers several advantages over prior studies, it also presents some limitations. First, due to the varied data formats and structures used by national public administrations, data preprocessing may vary by country, consequently impacting the time required to construct the corresponding cubical complexes. Second, the methodology does not, by itself, yield interpretative conclusions: as detailed in Section 2.4, once persistent homology is computed, a careful analysis of the resulting features is necessary to relate them to the underlying urban dynamics. Finally, our approach lacks a systematic methodology to reconcile persistent diagrams of different groups in order to extract conclusions.

Further variations of this method may be considered. Looking forward, it would be interesting to split the ‘city’ group into those who move to an adjacent neighbourhood and to the rest of the city. A similar refinement could be applied to the ‘outside’ group by distinguishing moves to adjacent regions, or even other countries. It would also be interesting to explore the outcome of this approach using more granular temporal resolution to determine if additional patterns emerge, although using a too high frequency, such as monthly, topological features may arise that are solely due to seasonality. Furthermore, it would also be interesting to study the socioeconomic features of the displaced population to enrich the persistent homology study. Finally, it would be beneficial to repeat the analysis in another city to further validate this approach.

REFERENCES

- [1] Erik J Amézquita, Michelle Y Quigley, Tim Ophelders, Jacob B Landis, Daniel Koenig, Elizabeth Munch, and Daniel H Chitwood. “Measuring hidden phenotype: quantifying the shape of barley seeds using the Euler characteristic transform”. In: *in silico Plants* 4.1 (Dec. 2021), diab033. ISSN: 2517-5025. DOI: [10.1093/insilicoplants/diab033](https://doi.org/10.1093/insilicoplants/diab033). eprint: <https://academic.oup.com/insilicoplants/article-pdf/4/1/diab033/42127695/diab033.pdf>. URL: <https://doi.org/10.1093/insilicoplants/diab033>.
- [2] Ayuntamiento de Madrid. *Acuerdo del Pleno, de 31 de mayo de 2017, por el que se aprueba la creación del Barrio denominado “Ensanche de Vallecas” en el distrito de Villa de Vallecas y la modificación del Reglamento Orgánico de los Distritos de la Ciudad de Madrid*. 140. Oct. 2017, pp. 156–162. URL: https://www.bocm.es/boletin/CM_Orden_BOCM/2017/06/14/BOCM-20170614-27.PDF.

- [3] Ayuntamiento de Madrid. *Acuerdo del Pleno, de 31 de octubre de 2017, por el que se aprueba la creación de los barrios “Casco Histórico de Vicálvaro”, “Valdebernardo”, “Valderrivas” y “El Cañaveral” y la delimitación territorial interna actualizada del Distrito de Vicálvaro, así como el cambio de denominación del “Barrio de San Andrés” por el de “Villaverde Alto, Casco Histórico de Villaverde” y la delimitación territorial interna actualizada del distrito de Villaverde, junto con la correspondiente modificación del Reglamento Orgánico de los Distritos de la Ciudad de Madrid*. 274. Nov. 2017, pp. 117–122. URL: https://www.bocm.es/boletin/CM_Orden_BOCM/2017/11/17/BOCM-20171117-48.PDF.
- [4] Ayuntamiento de Madrid. *Banco de Datos del Ayuntamiento de Madrid*. [Available at [Banco de Datos del Ayuntamiento de Madrid](https://servpub.madrid.es/CSEBD_WBINTER/inicio.html); downloaded April-2025]. 2025. URL: https://servpub.madrid.es/CSEBD_WBINTER/inicio.html.
- [5] Ayuntamiento de Madrid. *Geoportal del Ayuntamiento de Madrid*. [Available at [Geoportal del Ayuntamiento de Madrid](https://geoportal.madrid.es/IDEAM_WBGEOPORTAL/index.iam); downloaded April-2025]. 2025. URL: https://geoportal.madrid.es/IDEAM_WBGEOPORTAL/index.iam.
- [6] Ayuntamiento de Madrid. *Mapa de ruido 2006. Distrito 18 Villa de Vallecas*. 2006. URL: https://www.madrid.es/UnidadesDescentralizadas/Sostenibilidad/Ruido/MapaRuido/MapaRuido2006/Ficheros/Distrito_18_Villa_de_Vallecas.pdf.
- [7] Ayuntamiento de Madrid. *Mapa de ruido 2006. Distrito 19 Vicálvaro*. 2006. URL: https://www.madrid.es/UnidadesDescentralizadas/Sostenibilidad/Ruido/MapaRuido/MapaRuido2006/Ficheros/Distrito_19_Vicalvaro.pdf.
- [8] Nabil Baklouti, Bilel Gargouri, and Mohamed Jmaiel. “Towards patterns-based Linguistic Web Service composition”. In: *Computer Systems and Applications (AICCSA), 2015 IEEE/ACS 12th International Conference of*. IEEE. 2015, pp. 1–6.
- [9] Mikhail Belkin and Partha Niyogi. “Using manifold stucture for partially labeled classification”. In: *Advances in neural information processing systems*. 2002, pp. 929–936.
- [10] Michèle Belot and John Ermisch. “Friendship Ties and Geographical Mobility: Evidence from Great Britain”. In: *Journal of the Royal Statistical Society. Series A (Statistics in Society)* 172.2 (2009), pp. 427–442. ISSN: 09641998, 1467985X. URL: <http://www.jstor.org/stable/20622506> (visited on 12/09/2025).
- [11] Pierre Bérard, Gérard Besson, and Sylvain Gallot. “Embedding Riemannian manifolds by their heat kernel”. In: *Geometric & Functional Analysis GAFA* 4.4 (1994), pp. 373–398.
- [12] Bea Bleile, Adélie Garin, Teresa Heiss, Kelly Maggs, and Vanessa Robins. “The Persistent Homology of Dual Digital Image Constructions”. In: *Research in Computational Topology 2*. Ed. by Ellen Gasparovic, Vanessa Robins, and Katharine Turner. Cham: Springer International Publishing, 2022, pp. 1–26. ISBN: 978-3-030-95519-9. DOI: [10.1007/978-3-030-95519-9_1](https://doi.org/10.1007/978-3-030-95519-9_1). URL: https://doi.org/10.1007/978-3-030-95519-9_1.
- [13] Bea Bleile, Adélie Garin, Teresa Heiss, Kelly Maggs, and Vanessa Robins. “The persistent homology of dual digital image constructions”. In: *Research in computational topology 2*. Vol. 30. Assoc. Women Math. Ser. Springer, Cham, [2022] ©2022, pp. 1–26. ISBN: 978-3-030-95518-2; 978-3-030-95519-9. DOI: [10.1007/978-3-030-95519-9_1](https://doi.org/10.1007/978-3-030-95519-9_1). URL: https://doi.org/10.1007/978-3-030-95519-9_1.
- [14] Gunnar Carlsson. “Topology and data”. In: *Bull. Amer. Math. Soc. (N.S.)* 46.2 (2009), pp. 255–308. ISSN: 0273-0979. DOI: [10.1090/S0273-0979-09-01249-X](https://doi.org/10.1090/S0273-0979-09-01249-X). URL: <https://doi.org/10.1090/S0273-0979-09-01249-X>.
- [15] Maria Chiara Cavalleri, Nhung Luu, and Orsetta Causa. “Migration, housing and regional disparities: A gravity model of inter-regional migration with an application to selected OECD countries”. In: *OECD Economics Department Working Papers* 1691 (2021). DOI: [10.1787/421bf4aa-en](https://doi.org/10.1787/421bf4aa-en).

- [16] Seungho Choe and Sheela Ramanna. “Cubical Homology-Based Machine Learning: An Application in Image Classification”. In: *Axioms* 11.3 (2022). ISSN: 2075-1680. DOI: [10.3390/axioms11030112](https://doi.org/10.3390/axioms11030112). URL: <https://www.mdpi.com/2075-1680/11/3/112>.
- [17] Ronald R Coifman, Stephane Lafon, Ann B Lee, Mauro Maggioni, Boaz Nadler, Frederick Warner, and Steven W Zucker. “Geometric diffusions as a tool for harmonic analysis and structure definition of data: Diffusion maps”. In: *Proceedings of the National Academy of Sciences of the United States of America* 102.21 (2005), pp. 7426–7431.
- [18] Matthew Desmond and Carl Gershenson. “Who gets evicted? Assessing individual, neighborhood, and network factors”. In: *Social Science Research* 62 (2017), pp. 362–377. ISSN: 0049-089X. DOI: <https://doi.org/10.1016/j.ssresearch.2016.08.017>. URL: <https://www.sciencedirect.com/science/article/pii/S0049089X16300977>.
- [19] Matthew Desmond and Tracey Shollenberger. “Forced Displacement From Rental Housing: Prevalence and Neighborhood Consequences”. In: *Demography* 52 (Aug. 2015). DOI: [10.1007/s13524-015-0419-9](https://doi.org/10.1007/s13524-015-0419-9).
- [20] Lei Ding, Jackelyn Hwang, and Eileen Divringi. “Gentrification and residential mobility in Philadelphia”. In: *Regional Science and Urban Economics* 61 (2016), pp. 38–51. ISSN: 0166-0462. DOI: <https://doi.org/10.1016/j.regsciurbeco.2016.09.004>. URL: <https://www.sciencedirect.com/science/article/pii/S0166046216301223>.
- [21] NIAS Market Generated Displacement. “A Single City Case Study”. In: *National Institute for Advanced Studies: Washington, DC, USA* (1981).
- [22] Moon Duchin, Tom Needham, and Thomas Weighill. *The (homological) persistence of gerrymandering*. 2022. DOI: [10.3934/fods.2021007](https://doi.org/10.3934/fods.2021007). URL: <https://www.aims sciences.org/article/id/dd6624ea-7c57-4817-ac33-170a3acd9abe>.
- [23] Ingrid Ellen and Gerard Torrats-Espinosa. “Gentrification and Fair Housing: Does Gentrification Further Integration?” In: *Housing Policy Debate* 29 (Dec. 2018), pp. 1–17. DOI: [10.1080/10511482.2018.1524440](https://doi.org/10.1080/10511482.2018.1524440).
- [24] Ingrid Gould Ellen and Katherine M. O’Regan. “How low income neighborhoods change: Entry, exit, and enhancement”. In: *Regional Science and Urban Economics* 41.2 (2011), pp. 89–97. ISSN: 0166-0462. DOI: <https://doi.org/10.1016/j.regsciurbeco.2010.12.005>. URL: <https://www.sciencedirect.com/science/article/pii/S0166046211000044>.
- [25] Lance Freeman. “Displacement or Succession?: Residential Mobility in Gentrifying Neighborhoods”. In: *Urban Affairs Review* 40.4 (2005), pp. 463–491. DOI: [10.1177/1078087404273341](https://doi.org/10.1177/1078087404273341). eprint: <https://doi.org/10.1177/1078087404273341>. URL: <https://doi.org/10.1177/1078087404273341>.
- [26] Ori Friesen and Lori Ziegelmeier. *Understanding U.S. Racial Segregation Through Persistent Homology*. 2024. arXiv: [2410.10886 \[cs.SI\]](https://arxiv.org/abs/2410.10886). URL: <https://arxiv.org/abs/2410.10886>.
- [27] Robert Ghrist. “Barcodes: the persistent topology of data”. In: *Bull. Amer. Math. Soc. (N.S.)* 45.1 (2008), pp. 61–75. ISSN: 0273-0979. DOI: [10.1090/S0273-0979-07-01191-3](https://doi.org/10.1090/S0273-0979-07-01191-3). URL: <https://doi.org/10.1090/S0273-0979-07-01191-3>.
- [28] R.L. Glass. *London: Aspects of Change*. Report. MacGibbon & Kee, 1964. URL: <https://books.google.es/books?id=JfqftgEACAAJ>.
- [29] Allen Hatcher. *Algebraic topology*. Cambridge University Press, Cambridge, 2002, pp. xii+544. ISBN: 0-521-79160-X; 0-521-79540-0.
- [30] Abigail Hickok, Benjamin Jarman, Michael Johnson, Jiajie Luo, and Mason A. Porter. “Persistent Homology for Resource Coverage: A Case Study of Access to Polling Sites”. In: *SIAM Review* 66.3 (2024), pp. 481–500. DOI: [10.1137/22M150410X](https://doi.org/10.1137/22M150410X). eprint: <https://doi.org/10.1137/22M150410X>. URL: <https://doi.org/10.1137/22M150410X>.

- [31] Tomasz Kaczynski, Konstantin Mischaikow, and Marian Mrozek. *Computational homology*. Vol. 157. Applied Mathematical Sciences. Springer-Verlag, New York, 2004, pp. xviii+480. ISBN: 0-387-40853-3. DOI: [10.1007/b97315](https://doi.org/10.1007/b97315). URL: <https://doi.org/10.1007/b97315>.
- [32] Shizuo Kaji, Takeki Sudo, and Kazushi Ahara. *Cubical Ripser: Software for computing persistent homology of image and volume data*. 2020. arXiv: [2005.12692](https://arxiv.org/abs/2005.12692) [cs.CV]. URL: <https://arxiv.org/abs/2005.12692>.
- [33] Kamhon Kan. “Residential mobility and social capital”. In: *Journal of Urban Economics* 61.3 (2007), pp. 436–457. ISSN: 0094-1190. DOI: <https://doi.org/10.1016/j.jue.2006.07.005>. URL: <https://www.sciencedirect.com/science/article/pii/S0094119006000738>.
- [34] Peter Marcuse. “Gentrification, Abandonment, and Displacement: Connections, Causes, and Policy Responses in New York City”. In: *Journal of Urban and Contemporary Law* 28 (Jan. 1985).
- [35] Terra McKinnish, Randall Walsh, and T. Kirk White. “Who gentrifies low-income neighborhoods?” In: *Journal of Urban Economics* 67.2 (2010), pp. 180–193. ISSN: 0094-1190. DOI: <https://doi.org/10.1016/j.jue.2009.08.003>. URL: <https://www.sciencedirect.com/science/article/pii/S0094119009000588>.
- [36] Erin O’Neil and Sarah Tymochko. *Evaluating Cooling Center Coverage Using Persistent Homology of a Filtered Witness Complex*. 2025. arXiv: [2410.09067](https://arxiv.org/abs/2410.09067) [stat.AP]. URL: <https://arxiv.org/abs/2410.09067>.
- [37] Trond E Olsen and Gunnar Stensland. “On optimal timing of investment when cost components are additive and follow geometric diffusions”. In: *Journal of economic dynamics and control* 16.1 (1992), pp. 39–51.
- [38] Alex Pudlin. *Los Angeles Index of Displacement Pressure*. City of Los Angeles Open Data. Available at <https://geohub.lacity.org>. 2018. URL: https://geohub.lacity.org/datasets/70ed646893f642ddbca858c381471fa2_0/explore.
- [39] Ananya Shah. *A Comparison of Precinct and District Voting Data Using Persistent Homology to Identify Gerrymandering in North Carolina*. 2025. arXiv: [2506.13997](https://arxiv.org/abs/2506.13997) [cs.SI]. URL: <https://arxiv.org/abs/2506.13997>.
- [40] Mahesh Somashekhar. “Race, Class, and the Displacement of White Residents from Gentrifying U.S. Neighborhoods”. In: *Social Problems* (Nov. 2024), spae070. ISSN: 0037-7791. DOI: [10.1093/socpro/spae070](https://doi.org/10.1093/socpro/spae070). eprint: <https://academic.oup.com/socpro/advance-article-pdf/doi/10.1093/socpro/spae070/60811942/spae070.pdf>. URL: <https://doi.org/10.1093/socpro/spae070>.
- [41] Daniel Strömbom. *Persistent homology in the cubical setting: theory, implementations and applications*. 2007.
- [42] Andrea Varga and Andrew N Edmonds. “Multilingual extraction and editing of concept strings for the legal domain”. In: *Advances in Computer Science: an International Journal* 5.4 (2016), pp. 18–23.
- [43] Afra Zomorodian and Gunnar Carlsson. “Computing persistent homology”. In: *Discrete Comput. Geom.* 33.2 (2005), pp. 249–274. ISSN: 0179-5376. DOI: [10.1007/s00454-004-1146-y](https://doi.org/10.1007/s00454-004-1146-y). URL: <https://doi.org/10.1007/s00454-004-1146-y>.
- [44] Afra J. Zomorodian. *Topology for computing*. Vol. 16. Cambridge Monographs on Applied and Computational Mathematics. Cambridge University Press, Cambridge, 2005, pp. xiv+243. ISBN: 0-521-83666-2. DOI: [10.1017/CB09780511546945](https://doi.org/10.1017/CB09780511546945). URL: <https://doi.org/10.1017/CB09780511546945>.

Supporting Information

APPENDIX A. DATA

A.1. Datasets. The main data source for this study is the official demographic data of the city of Madrid. It is publicly available at [4], in CSV format. We used several tables, specifically those containing information about address changes. It can be found in the ‘C.Demografía y Población’ section, under ‘Padrón municipal/Dinámica geográfica/Cambios de domicilio en la ciudad’. We want to work with the finest spatial granularity possible. However, it is a requirement for us to know where individuals move from and to, as opposed to just the number of individuals arriving/leaving an area. We found that the latter is available at census tract level, whereas the former only at neighbourhood level. Therefore, we choose the tables in the aforementioned path containing data at neighbourhood level, and consider the whole period of time for which they are available: from 2004 until 2023.

In addition, we use several official shapefiles containing the geographical limits of the various administrative entities examined. All are available in [5]. The city of Madrid is divided into 21 districts, each uniquely identified with a number from 01 to 21; see Figure 10. Each of them is subdivided into 3 to 9 neighbourhoods, which, as of April 2025, total 131; see Figure 11. Each neighbourhood is assigned a three-digit number whose first two digits correspond to the district code. We refer to §A.2 for details on the changes the neighbourhoods underwent in the last two decades.

A.2. Data preprocessing. In this paper, we work with data from 2004 to 2023. During this period, the following neighbourhoods were officially created in 2017 and therefore appear in the dataset only from that year onward: Ensanche de Vallecas (district Villa de Vallecas), Valderrivas and El Cañaveral (district Vicálvaro). All of them were created as a result of two city council votings, see [2] and [3].

In 2017, district ‘19 Vicálvaro’ underwent several changes as a result of a new division into neighbourhoods [3]. Neighbourhoods ‘193 Valderrivas’ and ‘194 El Cañaveral’ were incorporated to the district, covering geographical areas that used to be part of neighbourhood ‘191 Casco Histórico de Vicálvaro’. Since these neighbourhoods were created in 2017, there is no emigration data available for these prior to this moment, in spite of the areas being populated before that date. Indeed, El Cañaveral was a “slum” that was torn down at the beginning of the 21st century and subsequently replaced by new urban developments. This means that people lived in this area long before its official incorporation as a separate neighbourhood, but were counted as part of neighbourhood ‘191 Casco Histórico de Vicálvaro’. Neighbourhood 192 is a different case. Until 2017 the number 192 corresponded to neighbourhood Ambroz, but also in 2017 Ambroz was removed and incorporated into ‘191 Casco Histórico de Vicálvaro’. Number 192 was then assigned to a new neighbourhood, called Valdebernardo. These changes must also be considered when quantifying the people who moved to/from this district.

At the turn of the century, the city of Madrid also expanded toward the South, resulting in an important growth of the district Villa de Vallecas. New housing developments were built in areas belonging to the Casco Histórico de Vallecas neighbourhood which were previously empty. Although the first inhabitants of these buildings moved there already in 2006, the new ‘183 Ensanche de Vallecas’ neighbourhood (literally ‘Expansion of Vallecas’) was scinded from Casco Histórico de Vallecas and officially recognised as an administrative independent neighbourhood in 2017 [2]. This is the reason why there is no data available for this neighbourhood until 2017.

The shapefile available on the Madrid city council website depicts the latest boundaries of the neighbourhoods. Thus, neighbourhoods that emerged later on as a result of splitting existing ones appear to have no emigration or immigration until that moment, creating the false impression that they were empty until then. Moreover, these neighbourhoods are located well inside the city and



FIGURE 10. Madrid map and their 21 districts as of April 2025.

not at the border, and leaving them blank until 2017 would severely interfere with the topology of the 3D cubical complexes we built.

As a consequence of the changes undergone in the neighbourhoods of these two districts, we perform the following modifications to the tabular data:

- From 2004 to 2016, we consider the whole district instead of individual neighbourhoods. We do so by assigning to each group we have split people moving into the same values to all the neighbourhoods in Vicálvaro (191, 192, 193 and 194), namely that obtained by merging 191 and 192 together. That is, someone moving within this district is considered to be staying in the same neighbourhood. By doing so, we ensure that no ‘holes’ are created in

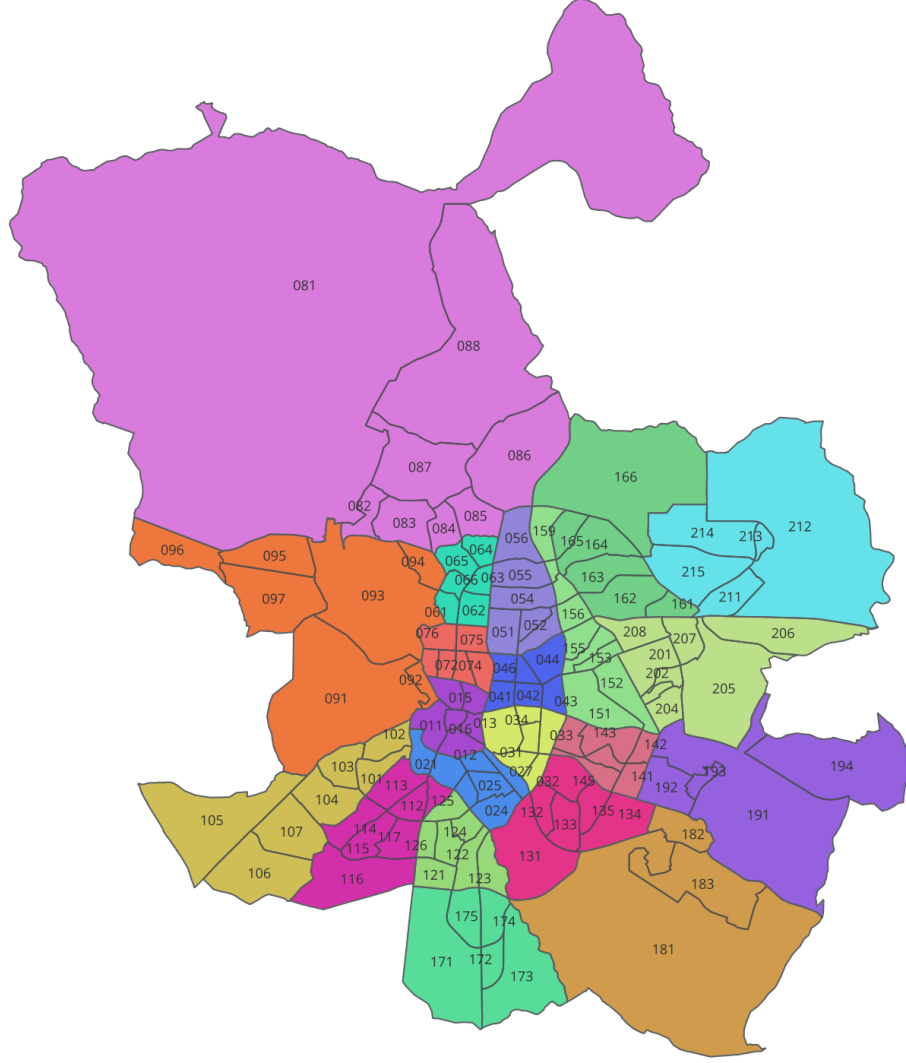


FIGURE 11. Madrid map and their 131 neighbourhoods as of April 2025, coloured by district.

the map in the areas where 193 and 194 are located, as well as that the change in location for 192 is correctly taken into account.

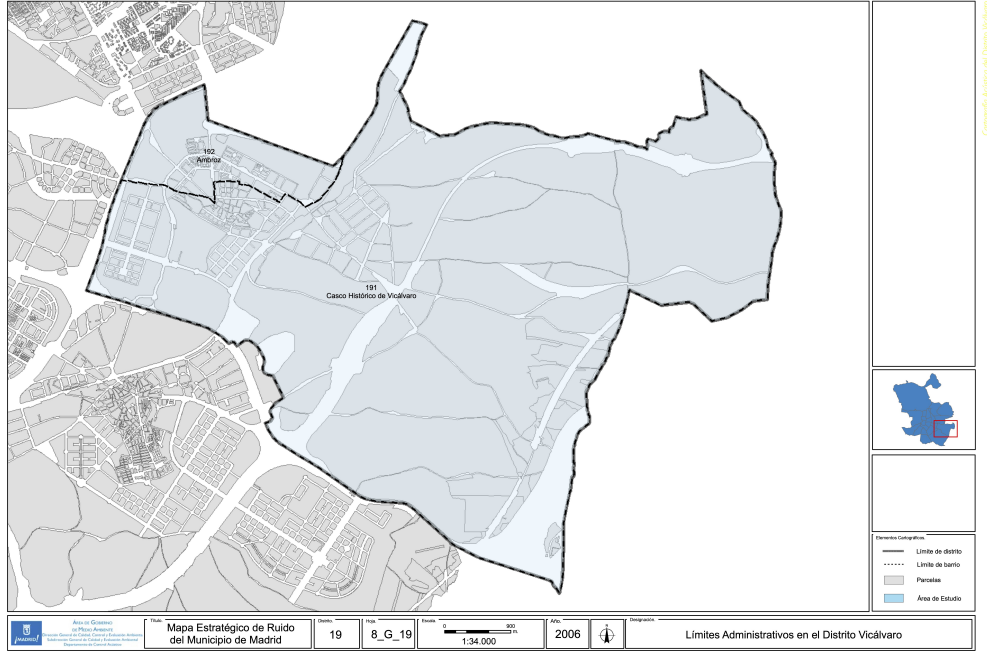
- From 2017 on, we keep data as is for the four neighbourhoods in district 19.
- We follow a similar approach to correctly deal with the creation of neighbourhood 183 Ensanche de Vallecas. As its area belonged to neighbourhood 181 Casco Histórico de Vallecas between 2004 and 2016, we assigning to it the emigration rates of 181 Casco Histórico de Vallecas during this period.

APPENDIX B. CUBICAL COMPLEXES

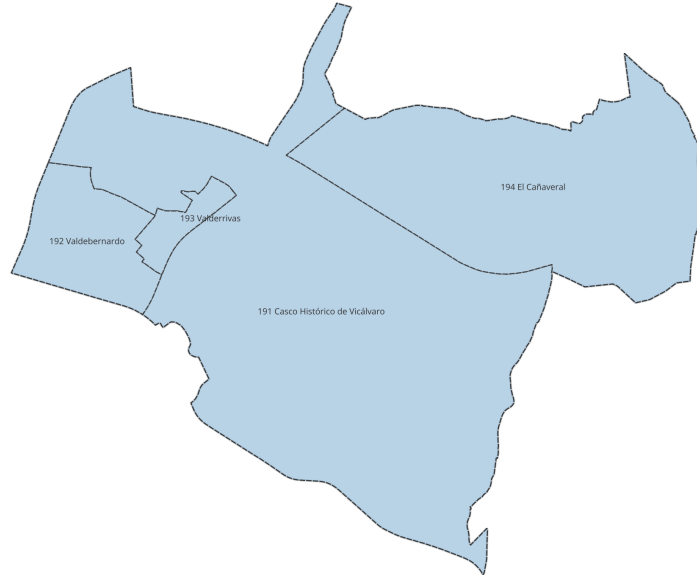
A d -dimensional grayscale digital image of size (n_1, n_2, \dots, n_d) is a real-valued function \mathcal{I} defined on a d -dimensional rectangular grid

$$I = \llbracket 1, n_1 \rrbracket \times \llbracket 1, n_2 \rrbracket \times \dots \times \llbracket 1, n_d \rrbracket \rightarrow \mathbb{R},$$

where $\llbracket 1, n_i \rrbracket$ is the set $\{k \in \mathbb{N} | 1 \leq k \leq n_i\}$.

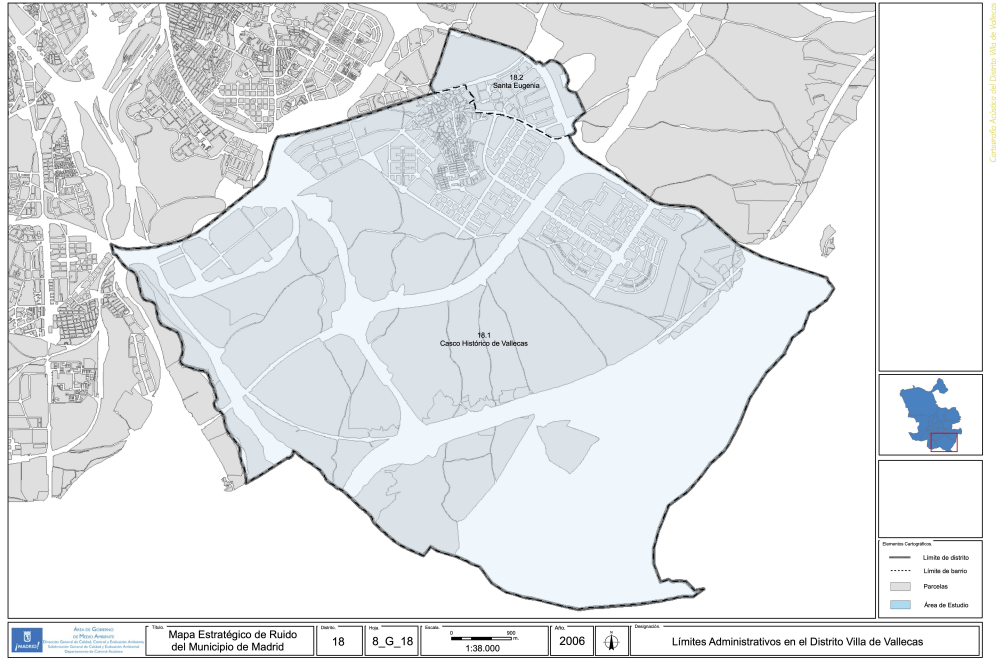


(A) Until 2017, Vicalvaro was made up of two neighbourhoods: Casco Histórico de Vicalvaro (191) and Ambroz (192). Map source: [7].

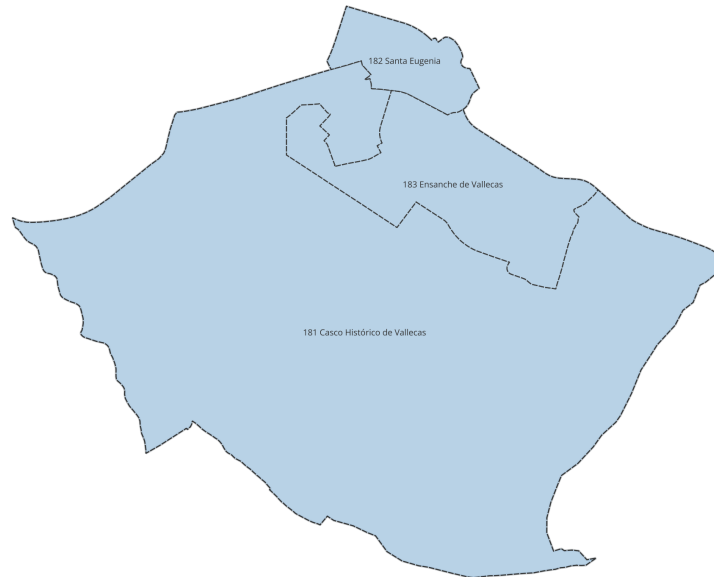


(B) From 2017 on, four neighbourhoods make up Vicalvaro [3]. Notice that neighbourhood no. 192 is no longer Ambroz but Valdebernardo.

FIGURE 12. Figures 12a and 12b depict the changes undergone in the neighbourhoods in district ‘19 Vicalvaro’ occurred in 2017. The district area remained unchanged, but the subdivision into neighbourhoods changed. On the top image it can be observed that in 2006, a large part of this district had not been developed yet.



(A) Villa de Vallecas district consisted only of two neighbourhoods until 2017. Map source: [6].



(B) Part of the area formerly covered by Casco Histórico de Vallecas neighbourhood was devoted to Ensanche de Vallecas in 2017 [2].

FIGURE 13. Figures 13a and 13b the changes in district ‘18 Villa de Vallecas’ in 2017. The district area remained unchanged, but the subdivision into neighbourhoods changed. On the top image it can be observed that in 2006, a large part of this district had not been developed yet.

Building on the analogy with digital photography, an element $p \in I$ called a pixel if $d = 2$ and a voxel if $d \geq 3$. Notice that with this construction voxels are also connected diagonally.

A cubical complex $X \subset \mathbb{R}^d$ is a cell complex consisting of a set of products of d intervals

$$\sigma = e_1 \times e_2 \times \dots \times e_d,$$

where e_i may be of the form $e_i = [l_i, l_i + 1]$ or of the form $e_i = [l_i, l_i]$ with $l_i \in \mathbb{Z}$ and such that all faces of $\sigma \in X$ are also in X .

There are two common ways to build a filtered cell complex from a grayscale image: the T- and the V-constructions. In the following, we recall the T-construction, implemented in this study. It follows a top-down approach to building a filtered cell complex. We refer to [12] for a comprehensive review of both constructions and for a series of duality results between them.

Given a d -dimensional grayscale digital image $\mathcal{I} : I \rightarrow \mathbb{R}$ of size (n_1, n_2, \dots, n_d) , the T-construction is the filtered cell complex (X, V) defined as:

- (1) X is a cubical complex built from the array of $n_1 \times \dots \times n_d$.
- (2) The d -cells $\tau^d \in X$ correspond exactly to the elements $p \in I$. We define the function V on X by extending \mathcal{I} to lower-dimensional cells σ by setting

$$V(\sigma) = \min_{\sigma \preceq \tau^d} (V(\tau^d)).$$

In other words, on a k -cube V takes the smallest value of all adjacent top-dimensional cubes.

In other words, each pixel is assigned a parameter value and is included in the filtration precisely when the filtration parameter attains that threshold. When a pixel is added to the filtration and one or more of its neighbours are already present, it adopts the minimum value of those neighbours for homological computation purposes.

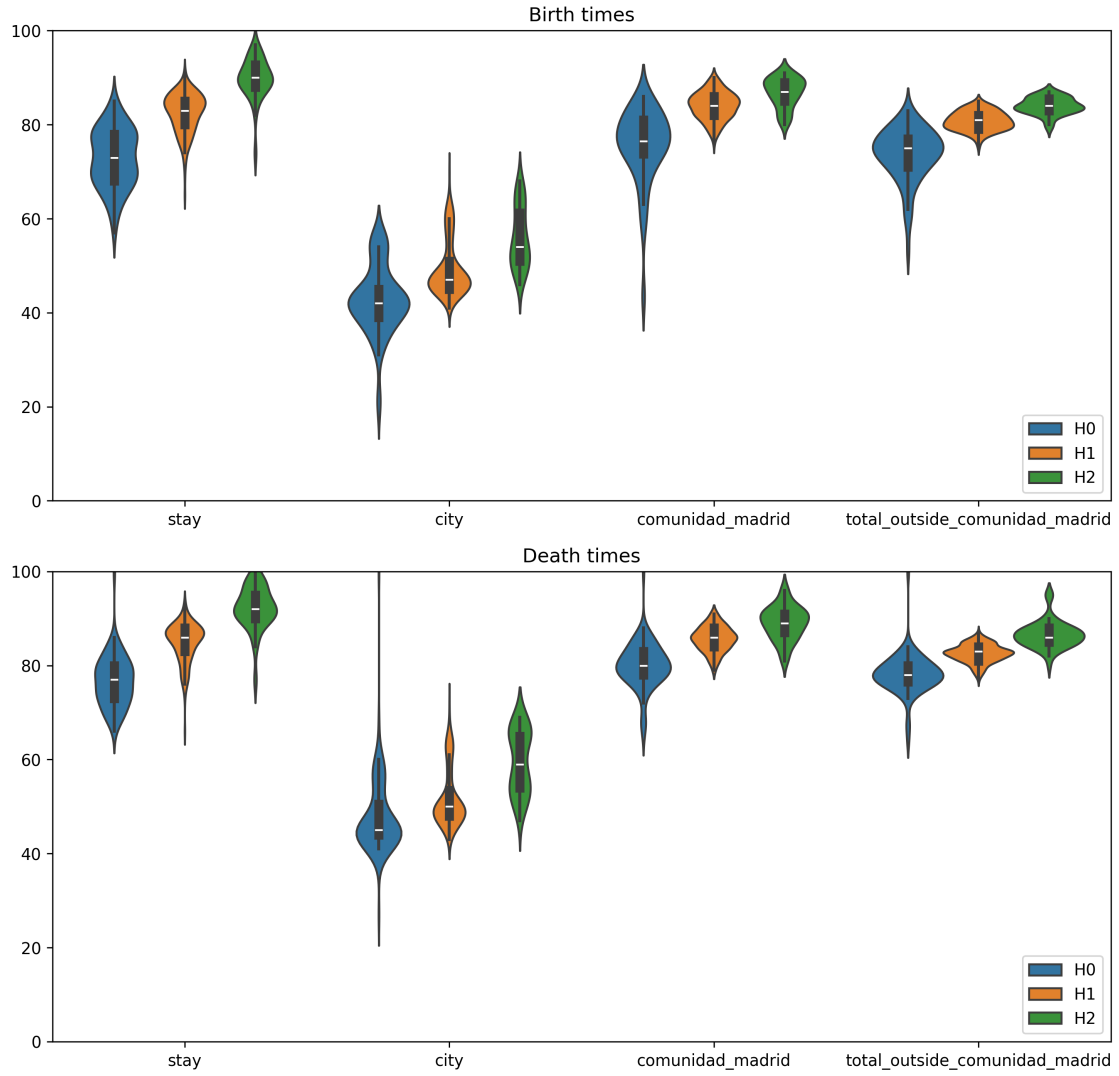


FIGURE 14. Violinplots of the distribution of the birth and death times of the topological features of each group.

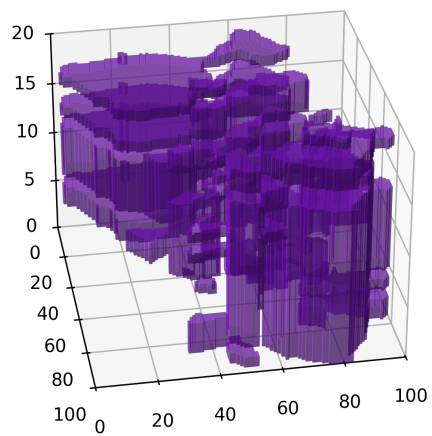
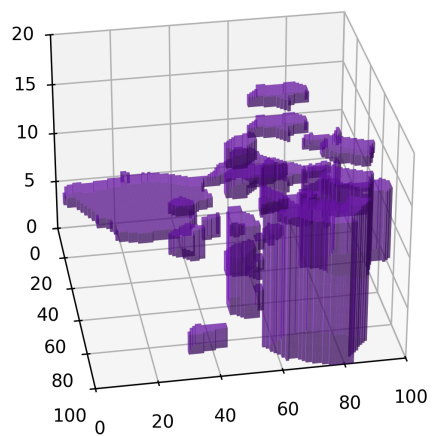
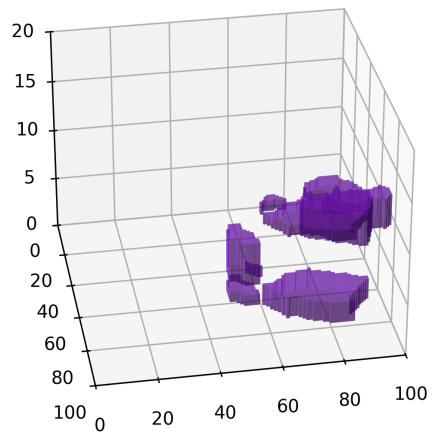


FIGURE 15. Cubical complexes for the group 'stay' at filtration-parameter values 65, 70 and 75.

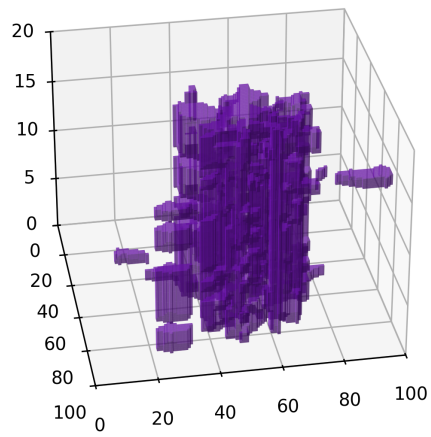
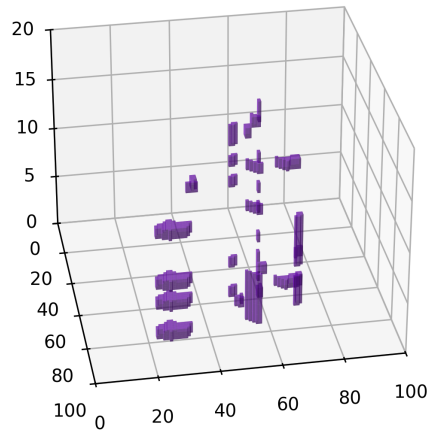
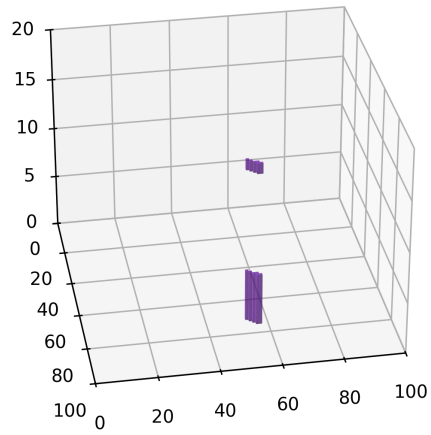


FIGURE 16. Cubical complexes for the group 'city' at filtration-parameter values 30, 40 and 50.

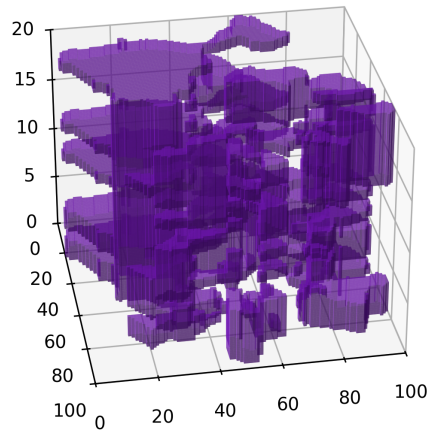
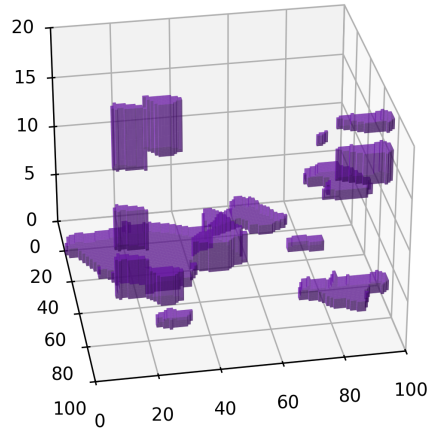
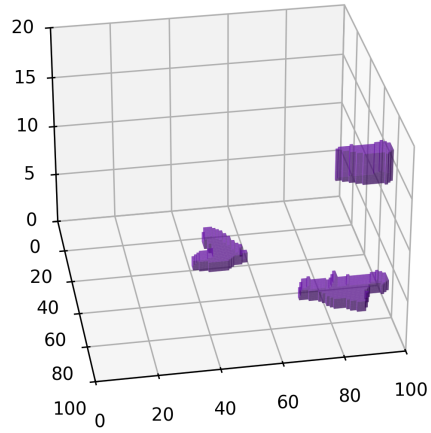


FIGURE 17. Cubical complexes for the group 'Comunidad de Madrid' at filtration-parameter values 60, 70 and 80.

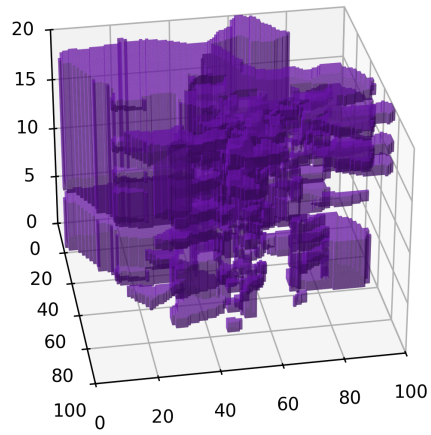
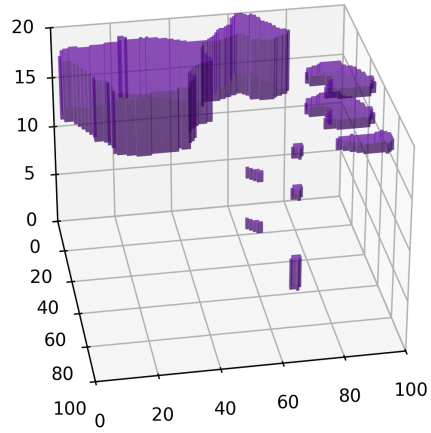
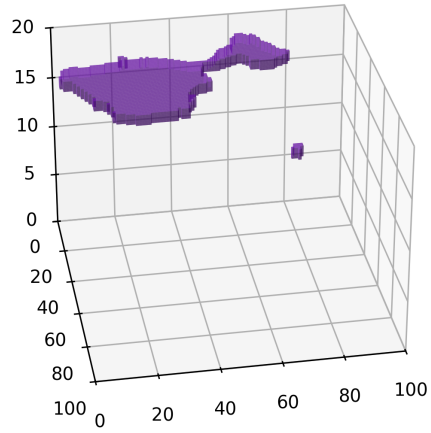


FIGURE 18. Cubical complexes for the group 'outside' at filtration-parameter values 60, 70 and 80.

	dim	measure	stay	city	C. Madrid	outside
birth	H0	mean	72.79	42.68	75.45	73.64
	H0	median	73.0	42.0	76.5	75.0
	H0	std	6.20	7.27	8.15	5.66
	H0	min	57.0	19.0	43.0	53.0
	H0	max	85.0	57.0	86.0	83.0
	H1	mean	82.53	49.31	84.04	80.80
	H1	median	83.0	47.0	84.0	81.0
	H1	std	4.19	5.82	2.93	2.02
	H1	min	65.0	41.0	76.0	75.0
	H1	max	91.0	70.0	90.0	85.0
	H2	mean	89.80	55.98	86.85	83.98
	H2	median	90.0	54.0	87.0	84.0
	H2	std	4.34	6.43	3.13	1.83
	H2	min	73.0	46.0	80.0	79.0
	H2	max	97.0	68.0	91.0	87.0
death	H0	mean	76.63	47.79	80.0123	78.13
	H0	median	77.0	45.0	80.0	78.0
	H0	std	5.466	8.23	4.94	4.28
	H0	min	66.0	27.0	65.0	64.0
	H0	max	100.0	100.0	100.0	100.0
	H1	mean	84.96	51.70	85.66	82.57
	H1	median	86.0	50.0	86.0	83.0
	H1	std	4.10	6.07	2.67	1.92
	H1	min	66.0	43.0	79.0	77.0
	H1	max	93.0	72.0	91.0	87.0
	H2	mean	92.18	59.5	89.02	86.58
	H2	median	92.0	59.0	89.0	86.0
	H2	std	4.56	6.70	3.55	2.85
	H2	min	76.0	47.0	81.0	80.0
	H2	max	100.0	69.0	96.0	95.0
persistence	H0	mean	3.83	5.10	4.565	4.49
	H0	median	2.0	3.0	2.0	3.0
	H0	std	5.51	8.93	7.89	6.36
	H0	min	1.0	1.0	1.0	1.0
	H0	max	43.0	81.0	57.0	47.0
	H1	mean	2.426	2.39	1.63	1.77
	H1	median	2.0	2.0	1.0	1.0
	H1	std	1.97	1.48	1.07	0.9
	H1	min	1.0	1.0	1.0	1.0
	H1	max	15.0	8.0	7.0	5.0
	H2	mean	2.38	3.53	2.17	2.6
	H2	median	2.0	2.0	2.0	2.0
	H2	std	1.68	3.26	1.84	2.44
	H2	min	1.0	1.0	1.0	1.0
	H2	max	9.0	16.0	9.0	12.0

TABLE 2. Descriptive statistics of the topological features obtained, by group and dimension.

dim	birth	death	persistence	year of birth	year of death	neighbourhood of birth	neighbourhood of death
0	57	100	43	2009		27	
0	60	74	14	2013	2011	171	132
0	64	78	14	2012	2020	212	107
0	65	75	10	2010	2012	81	81
0	67	77	10	2005	2008	86	86
0	61	70	9	2009	2014	181	131
0	64	73	9	2012	2015	164	212
0	71	80	9	2004	2006	83	87
0	66	73	7	2005	2007	116	171
0	62	68	6	2013	2011	194	181
1	78	93	15	2016	2019	205	158
1	77	86	9	2023	2022	95	95
1	78	87	9	2007	2008	164	166
1	69	77	8	2021	2020	191	191
1	78	86	8	2013	2013	201	203
1	79	87	8	2022	2020	159	159
1	81	89	8	2014	2013	62	16
1	72	79	7	2018	2018	181	174
1	78	85	7	2015	2010	125	25
1	79	86	7	2016	2015	24	122
2	89	98	9	2018	2019	25	27
2	90	97	7	2017	2015	13	27
2	85	91	6	2022	2020	193	193
2	92	98	6	2020	2019	13	27
2	89	94	5	2010	2012	93	82
2	93	98	5	2023	2020	141	141
2	95	100	5	2007	2008	27	27
2	86	90	4	2019	2018	193	193
2	88	92	4	2021	2020	101	101
2	89	93	4	2009	2010	208	208

TABLE 3. Top 10 most persistent features in each dimension for the group ‘stay’

dim	birth	death	persistence	year of birth	year of death	neighbourhood of birth	neighbourhood of death
0	19	100	81	2008		27	
0	22	45	23	2019	2018	27	26
0	35	58	23	2008	2009	106	105
0	46	68	22	2017	2016	194	191
0	39	53	14	2005	2006	106	106
0	31	44	13	2015	2013	27	16
0	39	52	13	2015	2013	106	106
0	32	43	11	2010	2006	142	43
0	33	43	10	2006	2006	158	62
0	34	44	10	2012	2022	158	54
1	57	65	8	2010	2009	214	213
1	41	48	7	2005	2007	35	31
1	44	51	7	2011	2010	32	31
1	57	64	7	2006	2007	214	213
1	45	51	6	2013	2012	25	26
1	51	57	6	2006	2007	163	164
1	57	63	6	2014	2015	214	213
1	62	68	6	2021	2021	96	95
1	43	48	5	2006	2006	154	52
1	44	49	5	2013	2013	66	51
2	49	65	16	2018	2018	31	27
2	54	65	11	2020	2020	31	27
2	56	65	9	2020	2020	131	27
2	56	65	9	2020	2020	134	141
2	51	59	8	2010	2009	31	27
2	58	65	7	2018	2018	181	27
2	59	66	7	2023	2013	165	164
2	60	65	5	2012	2013	205	207
2	48	52	4	2020	2017	126	111
2	50	54	4	2020	2020	71	76

TABLE 4. Top 10 most persistent features in each dimension for the group ‘city’

dim	birth	death	persistence	year of birth	year of death	neighbourhood of birth	neighbourhood of death
0	43	100	57	2004		88	
0	44	81	37	2018	2020	194	191
0	57	78	21	2006	2010	194	86
0	64	78	14	2013	2009	212	211
0	60	72	12	2010	2008	96	97
0	62	74	12	2020	2013	96	97
0	69	81	12	2021	2020	193	191
0	68	77	9	2007	2012	214	166
0	69	78	9	2006	2004	106	91
0	60	68	8	2004	2004	96	81
1	81	88	7	2020	2008	181	14
1	81	88	7	2014	2020	206	93
1	78	84	6	2012	2014	215	214
1	79	84	5	2005	2005	166	86
1	79	84	5	2011	2010	86	81
1	81	86	5	2018	2016	91	91
1	82	87	5	2010	2017	181	131
1	76	80	4	2005	2006	212	213
1	79	83	4	2009	2007	105	91
1	79	83	4	2004	2007	101	91
2	87	96	9	2009	2007	26	27
2	88	95	7	2012	2012	55	158
2	89	96	7	2009	2007	132	27
2	84	89	5	2012	2014	213	213
2	81	85	4	2004	2005	212	213
2	82	85	3	2011	2009	174	172
2	82	85	3	2018	2019	175	175
2	86	89	3	2011	2011	84	82
2	89	92	3	2015	2016	162	162
2	89	92	3	2021	2021	55	158

TABLE 5. Top 10 most persistent features in each dimension for the group ‘Comunidad de Madrid’

dim	birth	death	persistence	year of birth	year of death	neighbourhood of birth	neighbourhood of death
0	53	100	47	2020		141	
0	58	78	20	2021	2020	81	144
0	61	77	16	2020	2023	212	42
0	62	76	14	2018	2023	27	93
0	66	80	14	2016	2019	141	141
0	67	81	14	2009	2007	141	145
0	71	83	12	2018	2019	194	194
0	68	79	11	2020	2020	194	191
0	68	77	9	2013	2016	27	41
0	72	80	8	2004	2005	158	158
1	79	84	5	2012	2017	85	84
1	76	80	4	2020	2021	16	11
1	78	82	4	2009	2010	76	93
1	79	83	4	2023	2019	88	86
1	79	83	4	2020	2020	191	193
1	79	83	4	2023	2023	191	193
1	79	83	4	2015	2017	55	157
1	79	83	4	2008	2008	11	102
1	79	83	4	2005	2006	93	93
1	79	83	4	2023	2021	205	143
2	83	95	12	2014	2015	25	27
2	85	95	10	2009	2009	24	27
2	80	89	9	2019	2019	26	27
2	86	95	9	2015	2015	131	27
2	84	90	6	2011	2012	27	27
2	83	88	5	2023	2019	87	82
2	85	90	5	2017	2018	97	95
2	82	86	4	2017	2017	156	208
2	84	88	4	2008	2009	61	61
2	84	88	4	2021	2021	116	126

TABLE 6. Top 10 most persistent features in each dimension for the group ‘outside’